

1 **Reactivation-coupled brain stimulation enables complete learning generalization**

2 Yibo Xie^{1,2}, Minmin Wang³, Yuan Gao⁴, Baoyu Wu⁴, Shaomin Zhang², Mengyuan Gong⁴, Zoe
3 Kourtzi^{5,6}, Ke Jia^{1,7*}

4

5 ¹Liangzhu Laboratory, MOE Frontier Science Center for Brain Science and Brain-machine
6 Integration, State Key Laboratory of Brain-machine Intelligence, Zhejiang University,
7 Hangzhou, China

8 ²Interdisciplinary Institute of Neuroscience and Technology, College of Biomedical
9 Engineering & Instrument Science, Zhejiang University, Hangzhou, China

10 ³Westlake Institute for Optoelectronics, Westlake University, Hangzhou, China

11 ⁴Department of Psychology and Behavioral Sciences, Zhejiang University, Hangzhou, China

12 ⁵Department of Psychology, University of Cambridge, Cambridge, UK

13 ⁶Department of Psychology, Justus-Liebig University, Giessen, Germany

14 ⁷NHC and CAMS Key Laboratory of Medical Neurobiology, Zhejiang University, Hangzhou,
15 China

16

17 *Corresponding author:

18 Dr. Ke Jia

19 MOE Frontier Science Center for Brain Science and Brain-machine Integration, Zhejiang
20 University. Email: kjia@zju.edu.cn

21

22 **Abstract**

23 Generalization of learned knowledge to new contexts is essential for adaptive behavior. Despite
24 extensive research on the brain plasticity mechanisms underlying learning specificity, the
25 mechanisms that facilitate generalization remain poorly understood. Here, we investigate
26 whether using brain stimulation to disrupt offline consolidation in visual cortex promotes
27 learning generalization. Separate groups of participants ($N = 144$) were trained on visual
28 detection tasks using either a reactivation-based protocol or conventional full-practice,
29 combined with anodal or sham transcranial direct current stimulation (tDCS) over the visual
30 cortex. Strikingly, only combination of reactivation-based learning with anodal tDCS produced
31 complete generalization from trained to untrained stimuli, an effect consistently replicated
32 across features (orientation, motion direction). In contrast, reactivation-based learning alone
33 and conventional full-practice – whether with or without brain stimulation – yielded stimulus-
34 specific learning. Importantly, reactivation-coupled brain stimulation achieved generalization
35 with an 80% reduction in training trials while maintaining learning gains comparable to full-
36 practice. These findings demonstrate that reactivation and neuromodulation interact to unlock
37 learning generalization, revealing a key brain plasticity mechanism and offering a rapid,
38 translatable strategy for sensory rehabilitation.

39

40 **Keywords:** learning generalization | brain stimulation | memory reactivation | perceptual
41 learning

42

43 **Introduction**

44 Extensive practice over days to months can yield highly specialized skills, but the hallmark of
45 learning is generalization – an ability to transfer acquired skills flexibly to new contexts
46 (Shepard, 1987). Previous research has manipulated behavioral protocols to identify factors
47 that shape the degree of specificity and transfer, including task difficulty (Ahissar and
48 Hochstein, 1997; Jeter et al., 2009), training duration (Jeter et al., 2010), stimulus (Yashar and
49 Denison, 2017) and task variability (Manenti et al., 2023; Xiao et al., 2008). These strategies
50 can promote generalization, but often entail trade-offs: protocols that are simpler or shorter
51 tend to yield smaller learning gains, whereas those incorporating stimulus or task variability
52 often require training durations comparable to or exceeding that of conventional full-practice
53 regimens. Moreover, although such behavioral manipulations reveal empirical benefits, they
54 provide limited insight into the underlying neural mechanisms, leaving a critical gap in our
55 understanding of how brain plasticity supports the generalization of learning.

56 To address this gap, we focus on visual perceptual learning (VPL), a well-established
57 model of experience-dependent improvements in perceptual decisions (Watanabe and Sasaki,
58 2015). A hallmark of VPL is its high degree of stimulus specificity, a phenomenon thought to
59 reflect over-specialized neural representations in the visual cortex (i.e., perceptual overfitting)
60 (Sagi, 2011). This overfitting may arise due to learning either modifying feature representation
61 in early visual cortex (Jia et al., 2020, 2024; Yan et al., 2014) or enhancing read-out of sensory
62 neurons from early visual areas to optimize perceptual decisions (Dosher and Lu, 2017; Law
63 and Gold, 2008), with greater specificity emerging as training progresses. This creates a central
64 paradox in which extensive training is required to achieve substantial learning gains, yet such
65 training simultaneously drives overfitting that limits the generalizability of learning.

66 While improvements in conventional VPL primarily depend on prolonged online practice,
67 recent studies propose an alternative mechanism based on offline memory consolidation, which

68 may help resolve this paradox. Specifically, reactivation-based protocol uses brief reminder
69 trials to retrieve existing perceptual memories and enables learning via offline consolidation
70 processes. Although behavioral improvements – both in overall learning gains and in
71 specificity – are comparable between full-practice and reactivation-based VPL, evidence
72 indicates that the latter engages distinct brain plasticity processes. Specifically, these learning
73 gains are thought to arise from offline stabilization mediated by γ -aminobutyric acid (GABA)
74 (Eisenstein et al., 2023), the brain's primary inhibitory neurotransmitter. Anodal transcranial
75 direct current stimulation (tDCS), a non-invasive brain stimulation technique, has been shown
76 to reduce GABA concentrations in the visual cortex (Barron et al., 2016). Therefore, we
77 hypothesize that applying anodal tDCS to the visual cortex may disrupt perceptual overfitting
78 in reactivation-based VPL, thereby enhancing the generalization of learned perceptual skills.

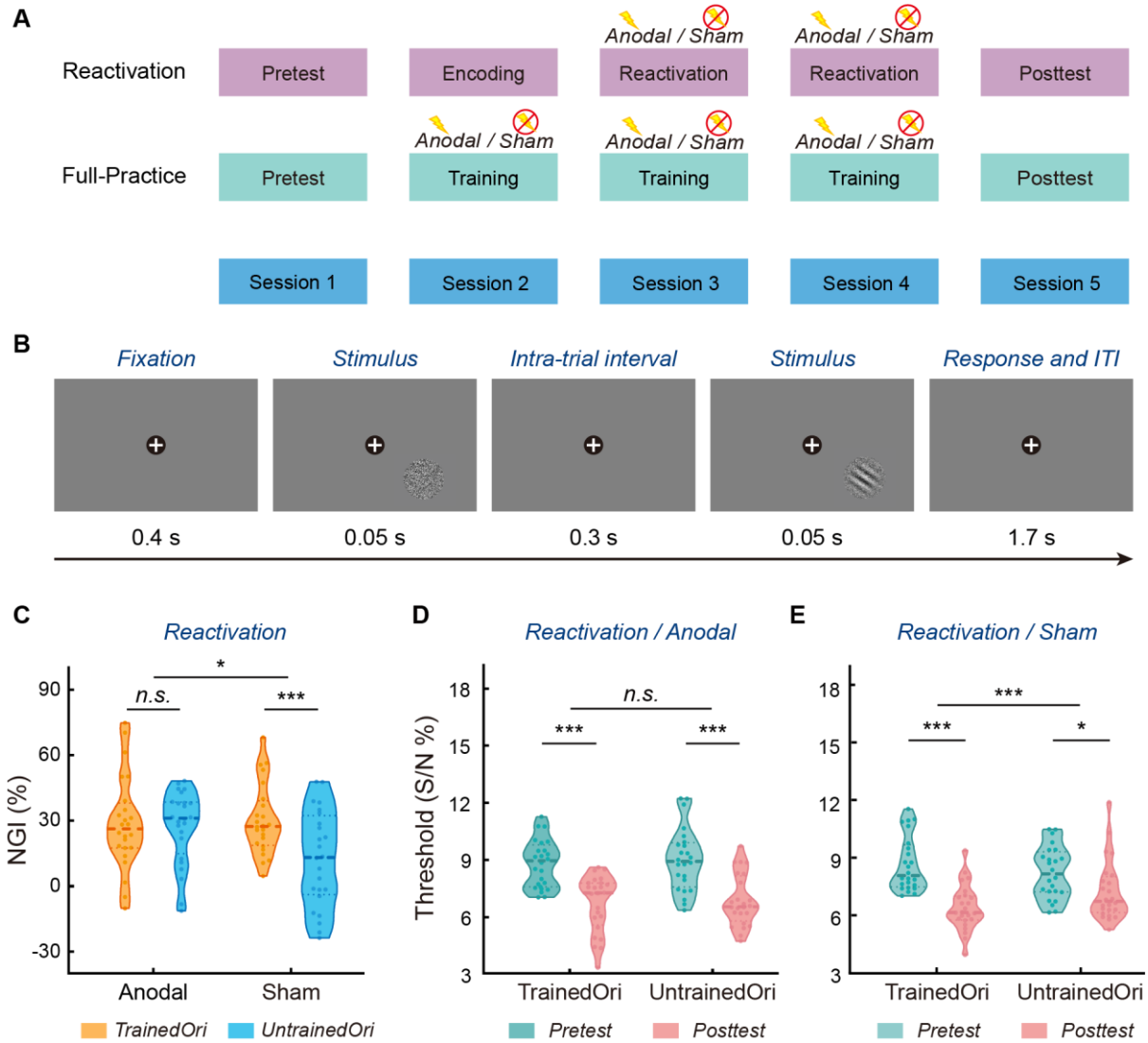
79 To test this hypothesis, we trained separate groups of participants on visual detection tasks
80 using either reactivation-based or full-practice protocols, combined with anodal or sham tDCS
81 over the visual cortex. Only combination of reactivation-based learning and anodal tDCS
82 produced complete transfer of learning from trained to untrained stimuli, an effect consistently
83 replicated across stimulus features (orientation, motion direction). In contrast, reactivation
84 alone or full-practice protocols resulted in stimulus-specific learning. These findings reveal a
85 key brain plasticity mechanism enabling generalization and suggesting a rapid, transferable
86 training strategy with direct relevance for clinical rehabilitation (e.g. sensory deficits).

87

88 **Results**

89 We trained forty-eight adults with a reactivation-based learning protocol (Bang et al., 2018),
90 using an orientation detection task (Figure 1A-B). On each trial, participants viewed two
91 sequentially presented stimuli and reported which interval contained the target (a Gabor patch
92 embedded in noise). Participants were randomly assigned to either the Anodal or Sham group

93 (N = 24 per group). The anodal electrode was placed over O1 (contralateral to the trained visual
 94 field) and the cathodal electrode over Cz (vertex), following the international 10-20 EEG
 95 system.



96 **Figure 1. Procedures and transfer effect using orientation task.**

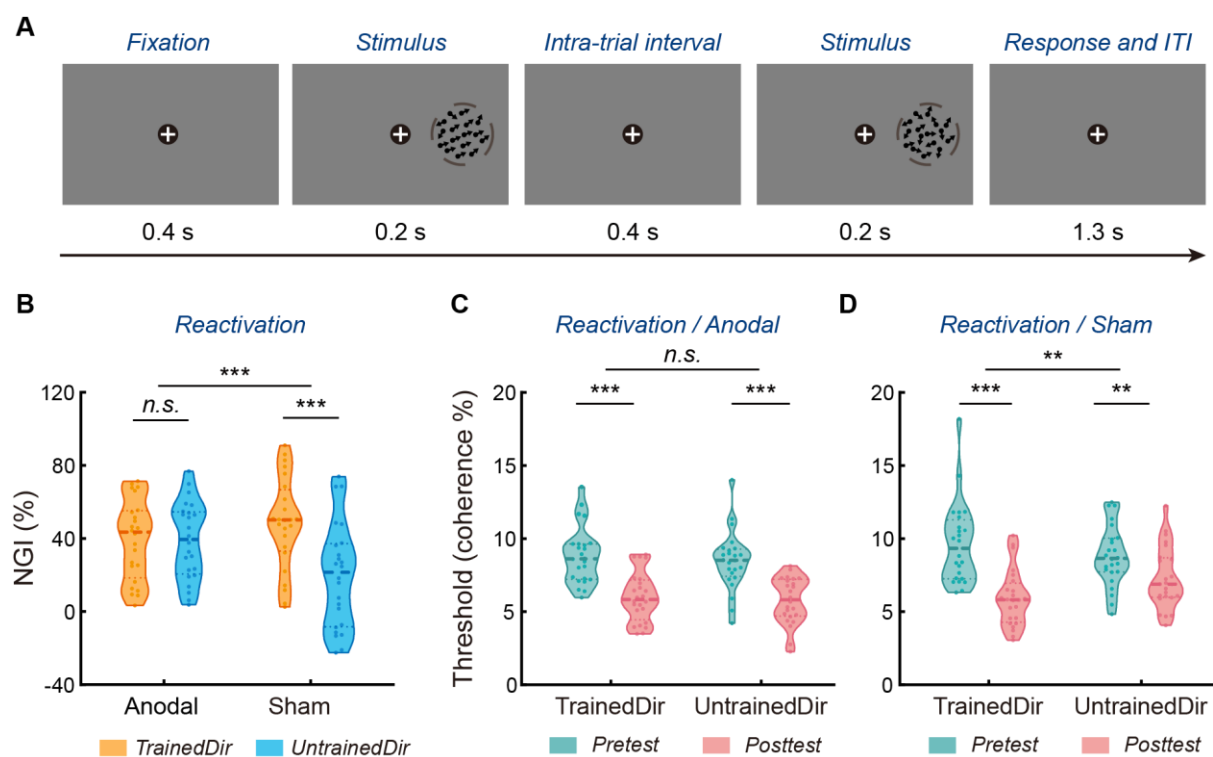
97 (A) Experimental design. Participants completed five sessions, including a pretest, training or
 98 reactivation, and a posttest. (B) Orientation detection task. Participants reported which of the two
 99 intervals contained the Gabor orientation. (C) Normalized learning gain index (NGI) for trained versus
 100 untrained orientations in the Reactivation (Anodal vs. Sham) groups. (D) Thresholds (S/N ratio) in
 101 *Reactivation/Anodal* group. A two-way repeated measures ANOVA (session: pretest vs. posttest ×
 102 orientation: trained vs. untrained) revealed a significant main effect of session ($F(1,23) = 124.406, p <$
 103 $0.001, \eta^2_p = 0.844$), but no interaction effect ($F(1,23) = 0.010, p = 0.923, BF_{01} = 3.633$), demonstrating

104 comparable learning for the trained (paired t-test: $t(23) = 7.338, p < 0.001$, Cohen's $d = 1.498$) and
105 untrained (paired t-test: $t(23) = 7.765, p < 0.001$, Cohen's $d = 1.585$) orientations. (E) Thresholds (S/N
106 ratio) in *Reactivation/Sham* group. A two-way repeated measures ANOVA (session: pretest vs. posttest
107 \times orientation: trained vs. untrained) revealed a significant interaction ($F(1,23) = 16.477, p < 0.001, \eta^2_p$
108 = 0.417), demonstrating stronger learning for the trained (paired t-test: $t(23) = 8.386, p < 0.001$, Cohen's
109 $d = 1.712$) compared to the untrained (paired t-test: $t(23) = 2.599, p = 0.016$, Cohen's $d = 0.531$)
110 orientation. The central lines in the box plot indicate the median values. The upper and lower lines
111 represent the interquartile range (25th – 75th percentiles). Each dot represents data from one participant.
112 * $p < 0.05$, *** $p < 0.001$, n.s. = not significant.

113
114 Our results showed complete transfer of learning in the *Reactivation/Anodal* group. In
115 contrast, we observed orientation-specific learning in the *Reactivation/Sham* group (Figure 1C),
116 consistent with previous studies (Amar-Halpert et al., 2017). To quantify the learning effects,
117 we calculated a normalized learning gain index ($NGI = [(Pre-test threshold - Post-test threshold)$
118 $/ ((Pre-test threshold + Post-test threshold) / 2)] \times 100\%$). A two-way mixed ANOVA
119 (stimulation condition: anodal vs. sham \times orientation: trained vs. untrained) on NGI revealed
120 a significant interaction ($F(1,46) = 5.551, p = 0.023, \eta^2_p = 0.108$). Post-hoc comparisons
121 showed significantly greater improvements for the trained over untrained orientation in the
122 *Reactivation/Sham* group (paired t-test: $t(23) = 4.484, p < 0.001$, Cohen's $d = 0.915$), but
123 comparable improvements across orientations in the *Reactivation/Anodal* group (paired t-test:
124 $t(23) = 0.213, p = 0.833, BF_{01} = 4.563$). Similar results were obtained when analyzing
125 thresholds (i.e., S/N ratio, Figure 1D-E). These findings indicate that reactivation-coupled
126 occipital stimulation promotes full transfer of learning.

127 To validate that the observed generalization was not specific to the orientation detection
128 task, we conducted a follow-up experiment using motion detection ($N = 48$, Figure 2A), while
129 keeping the task structure and stimulation protocols similar. A two-way mixed ANOVA
130 (stimulation condition: anodal vs. sham \times direction: trained vs. untrained) on NGI revealed a

131 significant interaction ($F(1,46) = 13.107$, $p < 0.001$, $\eta^2_p = 0.222$, Figure 2B). Post-hoc
 132 comparisons indicated that the Reactivation/Sham group exhibited significantly greater
 133 learning for the trained than untrained direction (paired t-test: $t(23) = 4.285$, $p < 0.001$, Cohen's
 134 $d = 0.875$), whereas the Reactivation/Anodal group showed equivalent improvements across
 135 directions (paired t-test: $t(23) = 0.117$, $p = 0.908$, $BF_{01} = 4.630$). Similar results were obtained
 136 when analyzing motion coherence (Figure 2C-D). This replication with a different stimulus
 137 feature corroborates our results showing that reactivation-coupled anodal stimulation enables
 138 complete transfer of perceptual learning.



139 **Figure 2. Transfer effect using motion detection task.**

140 (A) Motion detection task. Participants reported which of the two intervals contained the coherent
 141 motion dot field. (B) Normalized learning gain index (NGI) for the trained versus untrained direction
 142 in the Reactivation (Anodal vs. Sham) groups. (C) Thresholds (motion coherence) in
 143 *Reactivation/Anodal* group. A two-way repeated measures ANOVA (session: pretest vs. posttest \times
 144 direction: trained vs. untrained) revealed a significant main effect of session ($F(1,23) = 102.652$, $p <$
 145 0.001 , $\eta^2_p = 0.817$), but no interaction effect ($F(1,23) = 0.252$, $p = 0.621$, $BF_{01} = 3.239$), demonstrating
 146 comparable learning for the trained (paired t-test: $t(23) = 9.134$, $p < 0.001$, Cohen's $d = 1.864$) and

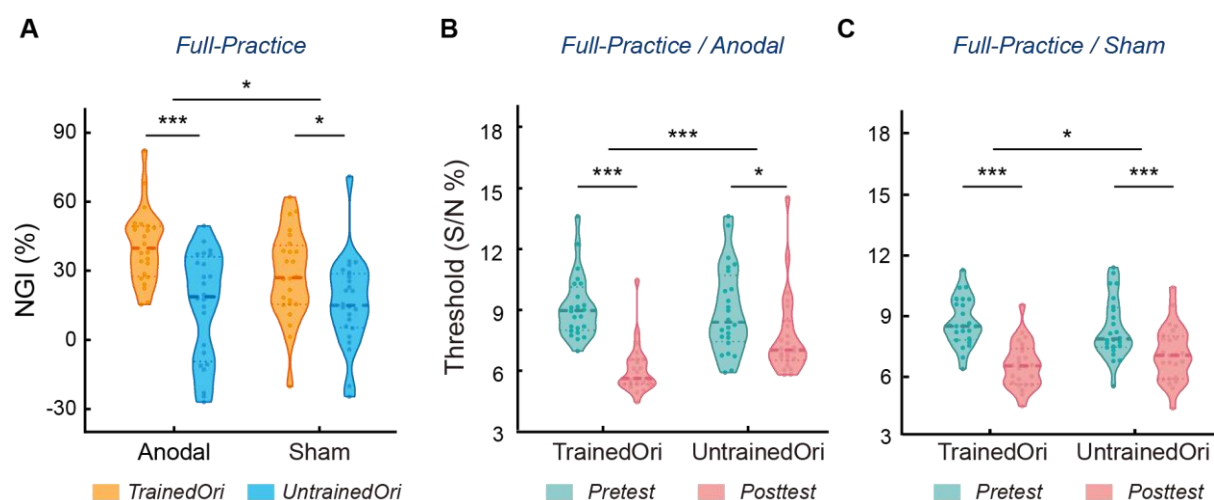
147 untrained (paired t-test: $t(23) = 8.973, p < 0.001$, Cohen's $d = 1.832$) directions. (D) Thresholds (motion
148 coherence) in *Reactivation/Sham* group. A two-way repeated measures ANOVA (session: pretest vs.
149 posttest \times orientation: trained vs. untrained) revealed a significant interaction ($F(1,23) = 9.864, p =$
150 $0.005, \eta^2_p = 0.300$), demonstrating larger learning effect for the trained (paired t-test: $t(23) = 7.764, p <$
151 0.001 , Cohen's $d = 1.585$) compared to the untrained (paired t-test: $t(23) = 3.244, p = 0.004$, Cohen's d
152 = 0.662) direction. The central lines in the box plot indicate the median values. The upper and lower
153 lines represent the interquartile range (25th – 75th percentiles). Each dot represents data from one
154 participant. ** $p < 0.01$, *** $p < 0.001$, n.s. = not significant.

155
156 We next asked whether the observed generalization in *Reactivation/Anodal* group might
157 reflect a reduced overall amount of learning. To test this possibility, we recruited an additional
158 group of 24 adults who completed standard full-practice with sham stimulation on the
159 orientation detection task (Figure 1A). A one-way ANOVA on NGI for the trained orientation
160 (group: *Reactivation/Anodal* vs. *Reactivation/Sham* vs. *Full-Practice/Sham*) revealed no
161 significant main effect of group ($F(2,69) = 0.085, p = 0.919$), which was further supported by
162 a Bayesian analysis ($BF_{01} = 7.952$; see Materials and Methods). Direct comparison confirmed
163 that the *Reactivation/Anodal* group attained learning gains comparable to those of the *Full-*
164 *Practice/Sham* group (independent t-test: $t(46) = 0.095, p = 0.925, BF_{01} = 3.467$). These results
165 suggest that the reactivation-coupled brain stimulation enhanced generalization without
166 compromising overall learning gains.

167 Next, we examined whether the observed generalization in *Reactivation/Anodal* group
168 could be attributed to reduced learning specificity inherent to the reactivation-based training
169 protocol itself. To address this, we conducted a two-way mixed ANOVA (group:
170 *Reactivation/Sham* vs. *Full-practice/Sham* \times orientation: trained vs. untrained) on NGI. The
171 analysis revealed a robust main effect of orientation ($F(1,46) = 21.870, p < 0.001, \eta^2_p = 0.322$),
172 but no significant effects of training protocol ($F(1,46) = 0.029, p = 0.866, BF_{01} = 3.486$) or their
173 interaction ($F(1,46) = 0.882, p = 0.352, BF_{01} = 2.302$). These results indicate that both the

174 Reactivation/Sham and Full-Practice/Sham groups showed a comparable degree of learning
175 specificity. Taken together with the performance in Reactivation/Anodal group, these findings
176 demonstrate that anodal tDCS is necessary for achieving enhanced generalization in
177 reactivation-based VPL.

178 Further, anodal tDCS combined with full-practice failed to enhance generalization;
179 instead, it increased learning specificity. We recruited another 24 adults and applied anodal
180 tDCS in combination with full-practice. A two-way mixed ANOVA (group: Full-
181 Practice/Anodal vs. Full-Practice/Sham \times orientation: trained vs. untrained) on NGI revealed
182 a significant interaction ($F(1,46) = 4.237, p = 0.045, \eta^2_p = 0.084$, Figure 3), indicating enhanced
183 specificity in the Full-Practice/Anodal group (i.e., larger improvements for the trained than
184 untrained orientation). Post-hoc comparisons showed that this increased specificity was driven
185 by greater gains for the trained orientation with anodal than sham tDCS (independent t-test:
186 $t(46) = 2.489, p = 0.017$, Cohen's $d = 0.718$), but no difference for the untrained orientation
187 (independent t-test: $t(46) = -0.246, p = 0.807$, $BF_{01} = 3.395$). These results indicate that anodal
188 tDCS combined with full-practice increased learning specificity, rather than enhancing
189 generalization.



190 **Figure 3. Full-Practice leads to learning specificity.**

191 (A) Normalized learning gain index (NGI) for the trained versus untrained orientation in the Full-

192 Practice (Anodal vs. Sham) groups. (B) Thresholds (S/N ratio) in Full-Practice/Anodal group. A two-
193 way repeated measures ANOVA (session: pretest vs. posttest \times orientation: trained vs. untrained)
194 revealed a significant interaction ($F(1,23) = 17.961, p < 0.001, \eta^2_p = 0.438$), demonstrating larger
195 learning effect for the trained (paired t-test: $t(23) = 10.689, p < 0.001$, Cohen's $d = 2.182$) compared to
196 the untrained (paired t-test: $t(23) = 2.782, p = 0.011$, Cohen's $d = 0.568$) orientation. (C) Thresholds
197 (S/N ratio) in Full-Practice/Sham group. A two-way repeated measures ANOVA (session: pretest vs.
198 posttest \times orientation: trained vs. untrained) revealed a significant interaction ($F(1,23) = 5.380, p =$
199 $0.030, \eta^2_p = 0.190$), demonstrating larger learning effect for the trained (paired t-test: $t(23) = 6.932, p <$
200 0.001 , Cohen's $d = 1.415$) compared to the untrained (paired t-test: $t(23) = 4.101, p < 0.001$, Cohen's d
201 $= 0.837$) orientation. The central lines in the box plot indicate the median values. The upper and lower
202 lines represent the interquartile range (25th – 75th percentiles). Each dot represents data from one
203 participant. * $p < 0.05$, *** $p < 0.001$, n.s. = not significant.

204
205 Lastly, to statistically validate the enhanced generalization in the Reactivation/Anodal
206 group compared with other groups, we calculated the NGI difference between the trained and
207 untrained orientation ($NGI\ difference = NGI_{trained} - NGI_{untrained}$), where lower values indicate
208 greater transfer and higher values indicate greater specificity. A two-way independent-
209 measures ANOVA (training protocol: reactivation vs. full-practice \times stimulation condition:
210 anodal vs. sham) on NGI difference showed a significant interaction ($F(1,92) = 9.755, p =$
211 $0.002, \eta^2_p = 0.096$). This pattern showed that Reactivation/Anodal enhanced generalization,
212 whereas Full-Practice/Anodal increased specificity. The divergence across protocols suggests
213 distinct neural mechanisms for reactivation-based versus repetition-based learning, consistent
214 with previous studies (Eisenstein et al., 2023; Kondat et al., 2024).

215

216 **Discussion**

217 Our study provides the first evidence that reactivation and neuromodulation interact to unlock
218 complete learning generalization. Reactivation-based protocols have been shown to result
219 mainly in learning specificity (Amar-Halpert et al., 2017), with a recent report suggesting

220 partial transfer (Kondat et al., 2025), consistent with the effects observed for the sham condition
221 in our study. In contrast, we demonstrate that reactivation-coupled anodal tDCS
222 enables complete learning transfer. We have replicated this result across two perceptual
223 detection tasks with different stimulus features (orientation, motion direction), providing
224 evidence for a perceptual plasticity mechanism that boosts generalization. In particular, our
225 protocol may disrupt the offline consolidation of learning in visual cortex – likely due to tDCS-
226 mediated GABA reduction – thereby reducing perceptual overfitting and promoting
227 generalization. This reduction in overfitting does not compromise learning gains, in line with
228 previous work suggesting that reactivation-based plasticity involves higher-order areas
229 (Kondat et al., 2024).

230 Previous studies on repetition-based learning have shown that different forms of electrical
231 stimulation can modulate learning outcomes in distinct ways. For instance, anodal or cathodal
232 stimulation alters VPL in a task-specific manner (Frangou et al., 2018), while stimulation at
233 alpha – but not theta or gamma – frequencies can enhance VPL improvements (He et al., 2022).
234 Consistent with these findings, the present study further demonstrated that anodal tDCS
235 selectively enhanced stimulus-specific learning. This pattern of results, that is distinct from that
236 observed in the reactivation groups, may be explained by two factors. First, prior research
237 suggests that excessive training in full-practice group can induce hyper-stabilization of memory
238 traces in the visual cortex (Shibata et al., 2017), a process that may rely less on offline
239 consolidation. As a result, the GABA reduction induced by anodal tDCS exerted a diminished
240 impact on consolidation-related processes. Second, anodal tDCS may increase the excitatory-
241 inhibitory (E-I) ratio (Barron et al., 2016) during training sessions, thereby promoting a more
242 plastic state in the visual cortex (Bang et al., 2018; Shibata et al., 2017) and enhancing stimulus-
243 specific learning gains in VPL following full practice. Future work is needed, integrating
244 multimodal neuroimaging (e.g., fMRI-MRS fusion) to directly investigate functional

245 reorganization and neurochemical plasticity in reactivation- versus repetition-based learning
246 (Jia et al., 2023, 2024).

247 In sum, we propose reactivation-coupled brain stimulation as a combined intervention
248 protocol for enhanced learning generalization at short training duration (i.e., reducing trial
249 numbers by 80%), while maintaining learning gains. As memory reactivation mechanisms
250 drive brain plasticity across multiple domains – including visual, motor, and mathematical
251 learning – our reactivation-coupled anodal tDCS protocol may offer a translatable solution for
252 clinical rehabilitation, enabling more efficient training with better generalization extending
253 beyond the specific training conditions.

254

255 **Materials and Methods**

256 **Participants**

257 Night-six participants took part in the reactivation-based VPL experiment. Half completed an
258 orientation detection task (main experiment; 21.71 ± 3.25 years old, 27 females) and half a
259 motion detection task (control experiment; 21.38 ± 2.14 years old, 28 females). Within each
260 task, participants were randomly assigned to the Reactivation/Anodal or the Reactivation/Sham
261 group ($N = 24$ for each group). Based on a previous perceptual learning study using similar
262 stimulation method (He et al., 2022), we conducted a prior independent t-test using the reported
263 effect size (Cohen's $d = 0.9$) in G*Power (Version 3.1) (Faul et al., 2007). This analysis
264 indicated that 24 participants per group would provide power greater than 85% to detect the
265 tDCS effect. Note that, this sample size was also comparable to prior tDCS studies on
266 perceptual learning (Frangou et al., 2018; He et al., 2022; Jia et al., 2022). In addition, we
267 recruited another forty-eight participants (22.00 ± 2.30 years old, 26 females) in the repetition-
268 based VPL experiment, and randomly assigned them to the Full-Practice/Anodal or the Full-
269 Practice/Sham group ($N = 24$ for each group). All participants were naïve to the purpose of the

270 study, had normal or corrected-to-normal vision, and reported being right-handed. Written
271 consent was obtained from all participants. The procedures used in this study were approved
272 by the Ethics Committee at Department of Psychology and Behavioral Sciences, Zhejiang
273 University (protocol number: 2022-061).

274

275 **Stimuli and apparatus**

276 Gabor patches (Gaussian windowed sinusoidal gratings) were presented in the lower-right
277 visual field at an eccentricity of 6.5° against a uniform gray background ($\sim 35 \text{ cd/m}^2$). The
278 Gabor stimuli had a diameter of 5° , random phase and spatial frequency of 1 cycle/degree. The
279 Gaussian envelope had standard deviation of 2.5° . Noise patterns from sinusoidal luminance
280 distributions were generated and superimposed on the Gabor patches at a specific signal-to-
281 noise (S/N) ratio. For instance, a 20% S/N ratio indicates that the noise pattern replaced 80%
282 of the pixels of the Gabor patch.

283 Random dot kinematograms (RDKs) were presented in an annular aperture located in the
284 right visual field at 8° eccentricity. Each display contained 400 dots (0.1° diameter) moving at
285 a speed of $10^\circ/\text{s}$. A specific proportion of dots moved coherently in one direction, while the
286 rest moved randomly. When a dot moved out of the aperture, it was wrapped around to reappear
287 from the opposite side along its motion direction.

288 The stimuli were generated using Psychtoolbox 3.0 (Brainard, 1997; Pelli, 1997)
289 implemented in MATLAB (The MATHWORKS Inc., Natick, MA, USA). Stimuli were
290 presented on a Dell Cathode-Ray Tube (CRT) monitor with the size of $40 \times 30 \text{ cm}^2$, resolution
291 of 1024×768 and a refresh rate of 60 Hz. Gamma correction was applied to the monitor. A
292 chin-rest was used to stabilize participants' head position and maintain the viewing distance at
293 72 cm.

294

295 **Experimental design and statistical analysis**

296 Participants trained with the reactivation-based protocol completed five sessions in the
297 following order: a pretest, an encoding session, two reactivation sessions, and a posttest. For
298 participants trained with repetition-based protocol, the encoding and reactivation sessions were
299 replaced with three standard full-practice training sessions (Figure 1A). All participants
300 performed two-interval forced-choice orientation detection tasks throughout these sessions.

301 *Orientation detection task.* As shown in Figure 1B, each trial began with a central fixation
302 cross (400 ms), followed by two sequential stimulus displays (50 ms each) separated by a 300
303 ms blank interval. One display contained a Gabor patch with specific S/N ratio, while the other
304 contained pure noise (0% S/N ratio), with presentation order randomized across trials.
305 Participants indicated which interval contained the Gabor patch via a keyboard press.

306 Participant's performance in the task was measured using a 2-down 1-up staircase with
307 10 reversals converging at 70.7% performance. In each staircase run, the S/N started with 15%
308 and adaptively changed with a step size of 0.05 log units. Each staircase run consisted of around
309 40 trials (1 – 2 mins). We calculated the thresholds as the geometric mean of the last six
310 reversals. The reference orientation was set at 55° for the trained stimulus and 125° for the
311 untrained stimuli, with these assignments counterbalanced across participants.

312 *Behavioral test session.* To stabilize fixation and familiarize participants with the task
313 before tests, they first completed a 30-trial practice run (20% S/N ratio, above threshold).
314 During practice run, auditory feedback was provided for incorrect responses. In both pretest
315 and posttest, they completed four staircase runs of the orientation detection task (two runs per
316 condition in random order). Detection thresholds were calculated by averaging the thresholds
317 from the two runs per condition. No feedback was provided during tests.

318 *Training session: Reactivation or Full-Practice.* All participants were trained on an
319 orientation detection task with fixed orientation and location throughout training sessions.

320 Auditory feedback was provided for incorrect trials. The Full-Practice group (i.e., repetition-
321 based VPL) completed three training sessions (16 staircase runs per session), while the
322 Reactivation group performed 16 staircases runs on the encoding session, followed by two
323 reactivation sessions, each consisting of three staircase runs. This design followed the protocol
324 of a prior study (Bang et al., 2018), while also matched the duration of the online stimulation
325 protocol (see *tDCS* section for details).

326 *Behavioral data analysis.* For each group and each orientation, we calculated a normalized
327 learning gain index ($NGI = [(Pre-test\ threshold - Post-test\ threshold) / ((Pre-test\ threshold +$
328 $Post-test\ threshold) / 2)] \times 100\ %$). Paired t-tests on NGI were used to compare performance
329 between trained and untrained orientations within participants. To examine differences across
330 multiple groups, we applied either independent t-tests or mixed ANOVAs on NGI. To quantify
331 the amount of transfer effects, we calculated the NGI difference between the trained and
332 untrained orientation ($NGI\ difference = NGI_{trained} - NGI_{untrained}$). Lower NGI difference reflects
333 more transfer, while higher NGI difference reflects greater specificity. A two-way independent-
334 measures ANOVA (training protocol \times stimulation condition) was applied on the NGI
335 difference. To evaluate the strength of evidence for the lack of significant effects, we conducted
336 parallel Bayesian analyses (Wagenmakers, 2007) using standard priors as implemented in
337 JASP Version 0.17.1.0 (JASP Team, 2023).

338 *Control experiment: motion detection task.* To examine the robustness of the generalizable
339 learning effect induced by reactivation-coupled brain stimulation, we replicated the
340 reactivation-based experiment with motion stimuli (RDKs). The behavioral task procedure was
341 similar to those used in the orientation detection task, with either anodal or sham stimulation.
342 On each trial, two sequential displays were presented: one contained a signal RDKs with a
343 given motion coherence, and the other was a noise field with 0% coherence (Figure 2A). The
344 reference direction was set at 60° for the trained stimulus and 300° for the untrained stimuli,

345 with these assignments counterbalanced across participants. Within each staircase run, the
346 initial motion coherence was set to 15% and was adjusted adaptively using a step size of 0.05
347 log units.

348 *Transcranial direct current stimulation* (tDCS). tDCS was delivered using a battery-
349 driven, constant current stimulator with a pair of rubber electrodes in a $5 \times 7 \text{ cm}^2$ saline-soaked
350 synthetic sponges. In the main experiments of orientation detection task , the anode electrode
351 was placed over the visual cortex (O1, 10-20 system) with conductive cream, while in the
352 control experiment of motion detection task, the anode electrode was placed approximately 3
353 cm above the mastoid–inion line and 5 cm left of the midline in the sagittal plane (left V5,
354 Battaglini et al., 2017). The cathode electrodes was positioned at the vertex (Cz) across
355 experiments. Stimulation parameters followed safety guidelines. For the anodal tDCS
356 condition, a direct current with an intensity of 1.5 mA was applied for 20 minutes, with a 30 s
357 fade in/out periods to minimize cutaneous sensations. We used online stimulation protocol (i.e.,
358 stimulation during training). In particular, the current flow was initiated 10 minutes before task
359 onset (rest period) and 10 minutes during the task. For the sham condition, participants received
360 a 30 s fade-in phase followed by a 30 s fade-out at the beginning and end of the stimulation
361 run, with no active stimulation in between. This sham protocol has been reported to effectively
362 keep participants blinded to the stimulation conditions (Gandiga et al., 2006).

363

364 **Acknowledgments**

365 This work was supported by grants to: K.J. from the National Natural Science Foundation of
366 China (32571225, 32300855) and the Non-profit Central Research Institute Fund of Chinese
367 Academy of Medical Sciences (2023-PT310-01). M.G. from National Natural Science
368 Foundation of China (32371087), Fundamental Research Funds for the Central University
369 (226-2024-00118), National Science and Technology Innovation 2030 — Major Project
370 2021ZD0200409. M.W. from National Natural Science Foundation of China (52407261), the
371 "Pioneer" and "Leading Goose" R&D Program of Zhejiang (2025C01137). Z.K. from the
372 Wellcome Trust (205067/Z/16/Z, 221633/Z/20/Z). For the purpose of open access, the authors
373 have applied for a CC BY public copyright license to any Author Accepted Manuscript version
374 arising from this submission.

375

376 **Author contributions:**

377 Y.X., M.G., and K.J. conceived the project and designed the experiments. Y.X., Y.G., B.W.,
378 and K.J. performed the experiments. Y.X., M.W., S.Z, and K.J. developed the tDCS protocols.
379 Y.X., M.G., and K.J. developed the analysis pipeline and analyzed the data. Y.X., K.Z., M.G.,
380 and K.J. wrote the manuscript.

381

382 **Declaration of interests:**

383 The authors declare no competing interests.

384

385

386 **References**

387 Ahissar M, Hochstein S. 1997. Task difficulty and the specificity of perceptual learning. *Nature*
388 **387**:401–406.

389 Amar-Halpert R, Laor-Maayany R, Nemni S, Rosenblatt JD, Censor N. 2017. Memory
390 reactivation improves visual perception. *Nat Neurosci* **20**:1325–1329.

391 Bang JW, Shibata K, Frank SM, Walsh EG, Greenlee MW, Watanabe T, Sasaki Y. 2018.
392 Consolidation and reconsolidation share behavioural and neurochemical mechanisms. *Nat
393 Hum Behav* **2**:507–513.

394 Barron HC, Vogels TP, Emir UE, Makin TR, O’Shea J, Clare S, Jbabdi S, Dolan RJ, Behrens
395 TEJ. 2016. Unmasking Latent Inhibitory Connections in Human Cortex to Reveal
396 Dormant Cortical Memories. *Neuron* **90**:191–203.

397 Battaglini L, Noventa S, Casco C. 2017. Anodal and cathodal electrical stimulation over V5
398 improves motion perception by signal enhancement and noise reduction. *Brain Stimul*
399 **10**:773–779.

400 Brainard DH. 1997. The Psychophysics Toolbox. *Spat Vis* **10**:433–436.

401 Dosher B, Lu Z-L. 2017. Visual Perceptual Learning and Models. *Annu Rev Vis Sci* **3**:343–363.

402 Eisenstein T, Furman-Haran E, Tal A. 2023. Increased cortical inhibition following brief motor
403 memory reactivation supports reconsolidation and overnight offline learning gains. *Proc
404 Natl Acad Sci* **120**:1–10.

405 Faul F, Erdfelder E, Lang A-G, Buchner A. 2007. G*Power 3: A flexible statistical power
406 analysis program for the social, behavioral, and biomedical sciences. *Behav Res Methods*
407 **39**:175–191.

408 Frangou P, Correia M, Kourtzi Z. 2018. GABA, not BOLD, reveals dissociable learning-
409 dependent plasticity mechanisms in the human brain. *Elife* **7**:1–22.

410 Gandiga PC, Hummel FC, Cohen LG. 2006. Transcranial DC stimulation (tDCS): A tool for
411 double-blind sham-controlled clinical studies in brain stimulation. *Clin Neurophysiol*
412 **117**:845–850.

413 He Q, Yang XY, Gong B, Bi K, Fang F. 2022. Boosting visual perceptual learning by
414 transcranial alternating current stimulation over the visual cortex at alpha frequency.
415 *Brain Stimul* **15**:546–553.

416 Jeter PE, Dosher BA, Liu SH, Lu ZL. 2010. Specificity of perceptual learning increases with
417 increased training. *Vision Res* **50**:1928–1940.

418 Jeter PE, Dosher BA, Petrov AA, Lu Z. 2009. Task precision at transfer determines specificity
419 of perceptual learning. *J Vis* **9**:1–13.

420 Jia K, Frangou P, Karlaftis VM, Ziminski JJ, Giorgio J, Rideaux R, Zamboni E, Hodgson V,
421 Emir U, Kourtzi Z. 2022. Neurochemical and functional interactions for improved
422 perceptual decisions through training. *J Neurophysiol* **127**:900–912.

423 Jia K, Goebel R, Kourtzi Z. 2023. Ultra-High Field Imaging of Human Visual Cognition. *Annu
424 Rev Vis Sci* **9**:479–500.

425 Jia K, Wang M, Steinwurzel C, Ziminski JJ, Xi Y, Emir U, Kourtzi Z. 2024. Recurrent
426 inhibition refines mental templates to optimize perceptual decisions. *Sci Adv* **10**:1–9.

427 Jia K, Zamboni E, Kemper V, Rua C, Goncalves NR, Ng AKT, Rodgers CT, Williams G,
428 Goebel R, Kourtzi Z. 2020. Recurrent Processing Drives Perceptual Plasticity. *Curr Biol*
429 **30**:4177–4187.e4.

430 Kondat T, Sasaki Y, Watanabe T, Censor N. 2025. Brief memory reactivations enable
431 generalization of offline visual perceptual learning mechanisms. *Sci Rep* **15**:1–9.

432 Kondat T, Tik N, Sharon H, Tavor I, Censor N. 2024. Distinct Neural Plasticity Enhancing
433 Visual Perception. *J Neurosci* **44**:1–9.

434 Law C-T, Gold JI. 2008. Neural correlates of perceptual learning in a sensory-motor, but not a
435 sensory, cortical area. *Nat Neurosci* **11**:505–513.

436 Manenti GL, Dizaji AS, Schwiedrzik CM. 2023. Variability in training unlocks generalization
437 in visual perceptual learning through invariant representations. *Curr Biol* **33**:817–826.

438 Pelli DG. 1997. The VideoToolbox software for visual psychophysics: transforming numbers
439 into movies. *Spat Vis* **10**:437–442.

440 Sagi D. 2011. Perceptual learning in Vision Research. *Vision Res* **51**:1552–66.

441 Shepard RN. 1987. Toward a universal law of generalization for psychological science. *Science
442 (80-)* **237**:1317–1323.

443 Shibata K, Sasaki Y, Bang JW, Walsh EG, Machizawa MG, Tamaki M, Chang L-H, Watanabe
444 T. 2017. Overlearning hyperstabilizes a skill by rapidly making neurochemical processing
445 inhibitory-dominant. *Nat Neurosci* **20**:470–475.

446 Wagenmakers EJ. 2007. A practical solution to the pervasive problems of p values. *Psychon
447 Bull Rev* **14**:779–804.

448 Watanabe T, Sasaki Y. 2015. Perceptual Learning: Toward a Comprehensive Theory. *Annu
449 Rev Psychol* **66**:1–25.

450 Xiao L-Q, Zhang J-Y, Wang R, Klein SA, Levi DM, Yu C. 2008. Complete transfer of
451 perceptual learning across retinal locations enabled by double training. *Curr Biol*
452 **18**:1922–1926.

453 Yan Y, Rasch MJ, Chen M, Xiang X, Huang M, Wu S, Li W. 2014. Perceptual training
454 continuously refines neuronal population codes in primary visual cortex. *Nat Neurosci*
455 **17**:1380–1389.

456 Yashar A, Denison RN. 2017. Feature reliability determines specificity and transfer of
457 perceptual learning in orientation search. *PLoS Comput Biol* **13**:1–18.

458